Organic &
Biomolecular
Chemistry

Cite this: *Org. Biomol. Chem.*, 2011, **9**, 5997

www.rsc.org/obc

PAPER

Theoretical insights into the metal-free and formal [2 + 2 + 2] cycloaddition strategy *via* intramolecular cascade propargylic ene/Diels–Alder reactions with tautomerization†

Xinyao Li and Jiaxi Xu*

Received 17th February 2011, Accepted 3rd June 2011
DOI: 10.1039/c1ob05254c

A metal-free and formal [2 + 2 + 2] cycloaddition of triynes has emerged recently as a novel methodology for the synthesis of fused tricyclic compounds *via* an intramolecular cascade propargylic ene reaction, Diels–Alder cycloaddition and tautomerization. DFT calculations on three model systems reveal that the ene reaction with low distortion energy makes the metal-free strategy feasible and, as the rate-determining step, affects the regioselectivity of unsymmetric triynes. Furthermore, the types of final products depend on H-transfer during tautomerization after the Diels–Alder reaction. Generally, the different tethered atoms between the yne moieties are responsible for the different regioselectivities and the final products in the [2 + 2 + 2] cycloadditions. On the basis of a comprehensive theoretical investigation into the mechanism, triynes involving cyclic ynes have been designed and are predicted to react to afford fused tetracyclic products under milder conditions due to dramatically lower energy barriers and by altering the rate-determining step to the Diels–Alder reaction.

Introduction

[2 + 2 + 2] Cycloadditions of alkynes provide elegant methods for the construction of fused polycyclic compounds.[1] It was first discovered by Bertholet in 1866 for benzene formation *via* thermal cyclization of three acetylene molecules. However, this powerful strategy, specifically the transition-metal-catalyzed process as the dominating strategy,[2] has been developed for the trimerization reaction of alkynes since the consequent transition metal-catalyzed cyclotrimerization of acetylenes to benzene derivatives was reported by Reppe *et al.* in 1948.[3] Although there exists an extensive literature on [2 + 2 + 2] cycloaddition, only a few examples have been reported for purely thermal processes with harsh conditions.[4]

Recently, Ley *et al.*,[5] Roglans *et al.*,[6] and Danheiser *et al.*[7] successively reported formal and metal-free [2 + 2 + 2] cycloaddition strategies based on a cascade of two pericyclic processes under relatively mild conditions, which opens a new door to the heat-induced [2 + 2 + 2] cycloaddition of alkynes, complementing the well established transition-metal-catalyzed methodology as a powerful strategy. However, there is a debate about the mechanism. Ley *et al.* proposed a similar mechanism to that stated by Johnson *et al.*[4b] to account for the process, in which the bond formation initially occurred between two alkynes to generate a 1,4-diradical or several unusual strained and reactive intermediates, which were then trapped by the third alkyne to produce an aromatic ring. An analogous diradical mechanism was also proposed by Parsons *et al.* to interpret the cyclization of enediynes discovered in their laboratory.[8] However, Roglans *et al.* and Danheiser *et al.* proposed, on the basis of their own experimental work, that the reactions proceed *via* a sequential intramolecular propargylic ene[9,10]/[4 + 2] cycloaddition[11] cascade mechanism, rather than the pathway proposed by Ley and co-workers. In addition, Roglans *et al.* also performed DFT calculations to rationalize the mechanism of the [2 + 2 + 2] cycloaddition of their macrocyclic amine-containing triyne as a novel domino process.

To the best of our knowledge, this metal-free [2 + 2 + 2] cycloaddition strategy is still a new potential methodology, first discovered by Ley *et al.*[5] in 2005, with the following unsolved questions: a) which pathway is possible and feasible kinetically; b) which step is the rate-determining step; c) for unsymmetric triynes or their analogs, which two of the three yne bonds participate in the intramolecular propargylic ene reaction; d) why these reactions lead to different kinds of products; e) why this strategy does not need a transition metal catalyst; f) what is the effect of different substituents; g) what kind of substrates can be engaged under more mild conditions. The answers to these questions will not only provide a comprehensive and deep understanding on this novel metal-free [2 + 2 + 2] cycloaddition at the molecular level, but also guide further rational design of new useful strategies for the cascade reaction.

State Key Laboratory of Chemical Resource Engineering and Department of Organic Chemistry, Faculty of Science, Beijing University of Chemical Technology, Beijing 100029, China. E-mail: jxxu@mail.buct.edu.cn; Fax: +86 10 6443 5565; Tel: +86 10 6443 5565

† Electronic supplementary information (ESI) available: energies of all stable and saddle points, molecular modelling coordinates, and all calculation details. See DOI: 10.1039/c1ob05254c

Results and discussion

To probe the mechanism of the cascade reactions with an emphasis on understanding the mechanism, and to promote the application of the metal-free [2 + 2 + 2] cycloaddition, DFT calculations at the B3LYP/6-311+G(d,p) level of theory were performed on experimental model systems classified as three types with different results (Scheme 1) and our designed model systems. Singlet diradical intermediates[12] were located with UB3LYP/6-311+G(d,p). Solvent effects were computed using the CPCM model in toluene.

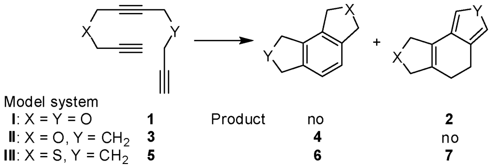

Scheme 1 [2 + 2 + 2] Cycloadditions of model systems **I–III**.

1. Three model systems

Calculations on the model system **I** show that the first step of the cascade reaction corresponds to an intramolecular propargylic ene-type reaction of a 1,6-diyne, permitting the six-electron pericyclic process, with suprafacial orbital interaction, to generate a vinylallene of type **8** (Fig. 1). This is exergonic by 35.5 kcal mol^{-1}, requiring an activation free energy of 30.3 kcal mol^{-1}. In the ene-type reaction transition structure **TS1**, the forming C–C bond distance is 2.06 Å, while the forming and breaking C–H bond distances are 1.59 and 1.25 Å, respectively (Fig. 2). In Ley's originally proposed mechanism, either a diradical species or a cyclobutadiene intermediate was proposed through the reaction processes. However, calculations show that the diradical intermediate with a computed $<S^2>$ of 1.04 is highly energy-demanding with a free energy of 40.1 kcal mol^{-1}, revealing that the diradical pathway is not feasible. Unfortunately, the transitions state (TS0) to the diradical intermediate was not located, which would stand at a higher energy level.

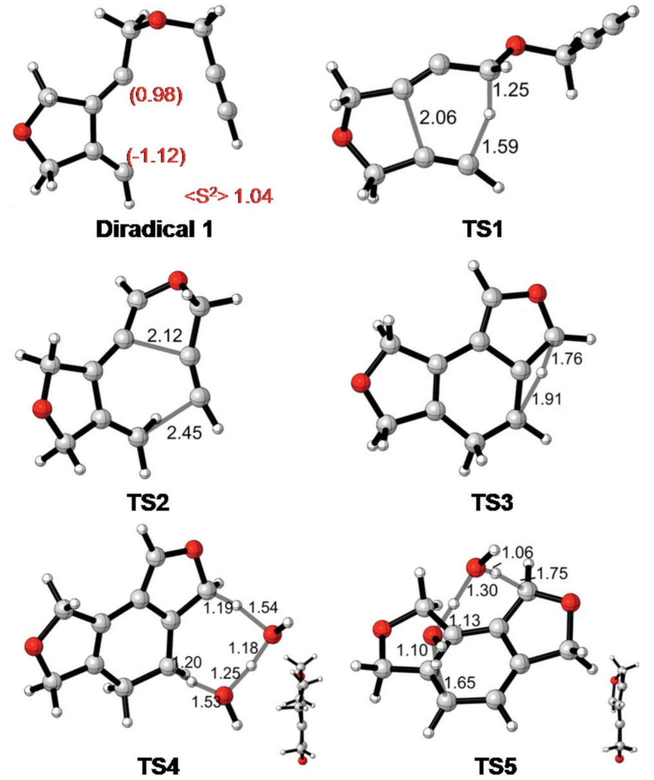

Fig. 2 Diradical intermediate structure with spin distribution (red numbers) and transition state structures in model system **I**. Selected distances shown in Å.

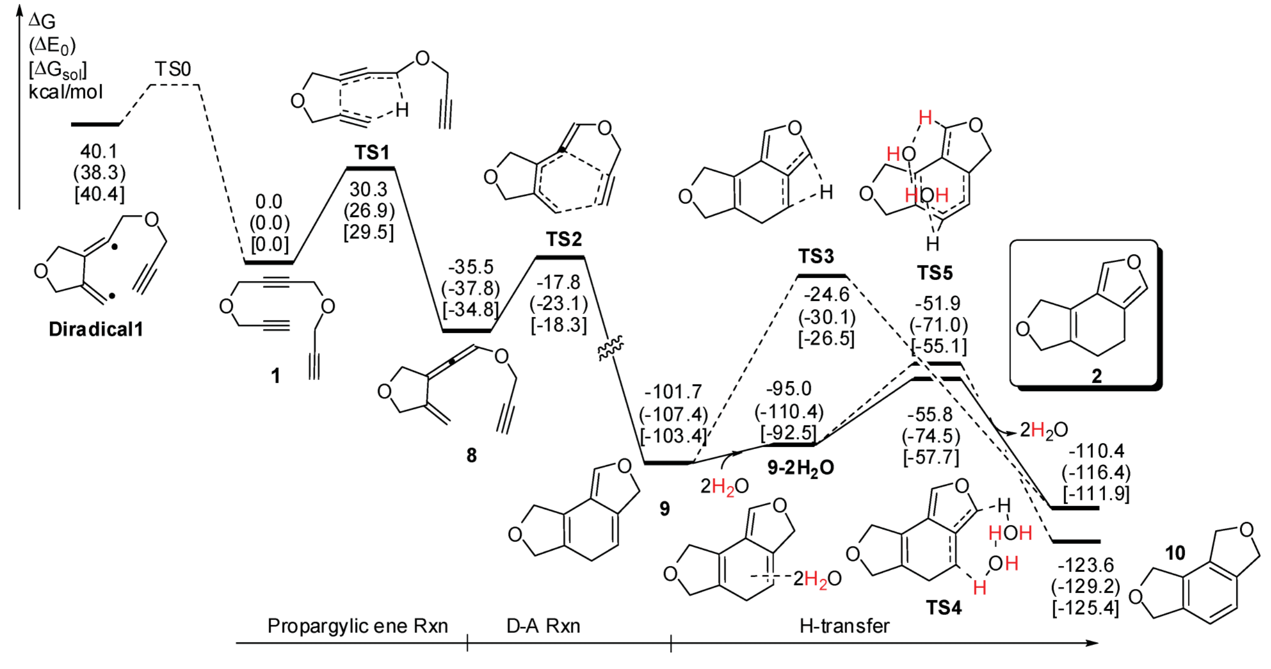

Fig. 1 DFT computed energy surface for the metal-free [2 + 2 + 2] cycloaddition of model system **I**.

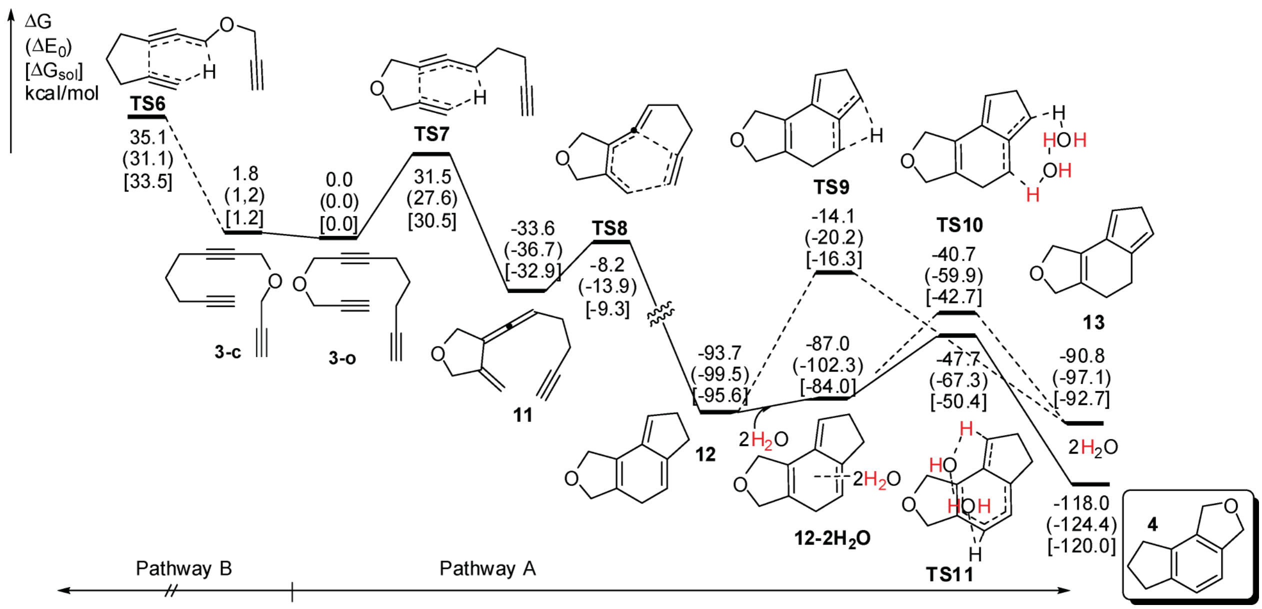

Fig. 3 DFT computed energy surface for the metal-free [2 + 2 + 2] cycloaddition of model system **II**.

The subsequent step is an intramolecular Diels–Alder (D–A) reaction with an activation free energy of 17.7 kcal mol^{-1}, in which the alkyne moiety serves as a dienophile and the vinylallene moiety serves as a diene. In **TS2**, the two forming C–C bond distances are different (2.12 Å *versus* 2.45 Å, Fig. 2), indicating that the intramolecular D–A reaction occurs in a concerted but asynchronous fashion.[13] Once the intramolecular D–A adduct **9** is generated *via* a highly exergonic process, the following tautomerization is required. A thermal [1,3]-H-transfer through **TS3** with a suprafacial orbital interaction with a high barrier (77.1 kcal mol^{-1}) was rejected due to the extremely strained four-membered ring formed in the TS and inhibition of the orbital symmetry. While a thermal [1,5]-H-transfer TS was not located because a six-membered ring transition state cannot be generated due to the rigidity of the planar conjugated diene moiety although the orbital symmetry is allowed. However, as water was referred to in Ley's experiment[5] and the water-participated H-transfer was proven experimentally by Roglans *et al.*,[6] herein, added water molecules can indeed assist the H-transfer with a much lower barrier through two competing pathways, in which an eight-membered ring H-transfer assisted by two water molecules (**TS4**) is 3.9 kcal mol^{-1} lower in activation free energy than a ten-membered ring H-transfer (39.2 *versus* 43.1 kcal mol^{-1}), due to the existence of the aromatic π bond of the furan ring in **TS4** and the disfavored twist strain in **TS5** resulted from the rigidly planar conjugated diene (H-transfer assisted by a water molecule has also been computed with higher energy level, which lies at −47.7 and −39.4 kcal mol^{-1}, respectively. See supporting information for details). So furan-type product **2** is the kinetically accessible product despite the fact that **10** is the more stable product as both H-transfer processes are irreversible, which is in good agreement with Ley's experiment. Reviewing the whole energy surface of the cascade reaction, we found that the rate-determining step is the ene reaction, while the D–A reaction is relatively facile. Besides, the H-transfer processes determine the types of final products.

The computed energy surface for the model system **II** is given in Fig. 3. Different from the model system **I**, this reaction can proceed *via* two pathways as the triyne **3** is an unsymmetric triyne (pathways A and B, Fig. 3). Calculations show the regioselectivity in that the triyne **3** has two reactive conformers, in which two geometrically close alkynes are tethered by a carbon atom in **3-c**, or by an oxygen atom in **3-o** (Fig. 3 and 4). The angle C2–C3–C4 in **3-c** is close to the angle C7–O8–C9 in **3-o** (115.6° and 115.5°). However, the bond distances of C2–C3 and C3–C4 in **3-c** are longer than those of C7–O8 and O8–C9 in **3-o** (1.54 *versus* 1.43 or 1.42 Å), directly leading to the longer C1–C5 bond in **3-c** than C6–C10 in **3-o**. The conformer **3-o**, characterised by two closer

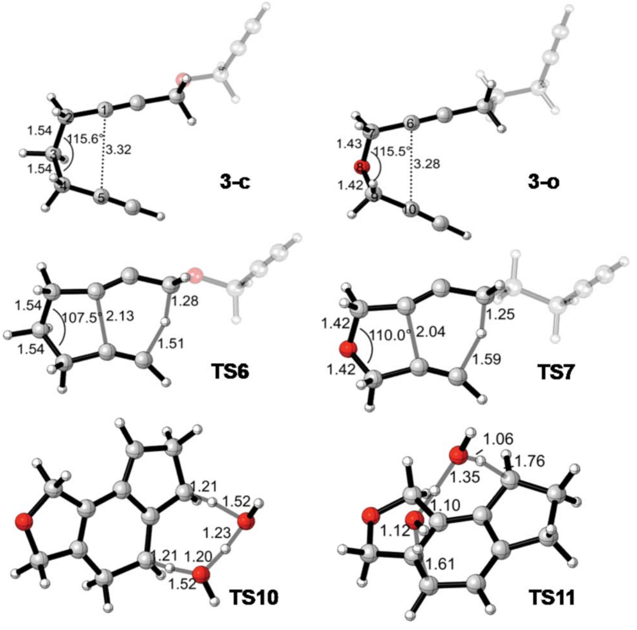

Fig. 4 Transition state structures in model system **II**. Selected distances shown in Å.

alkynes, served as a more reactive conformer, and is 1.8 kcal mol^{-1} more stable than **3-c**. Two transition states of the ene reaction were located from the two conformers. The change of the angle C2–C3–C4 from 115.6° (**3-c**) to 107.5° (**TS6**) is greater compared to that of C7–O8–C9 from 115.5° (**3-o**) to 110.0° (**TS7**), implying that **TS6** bears more ring strain. Additionally, the C1–C5 bond in **TS6** is 2.13 Å, 0.09 Å longer than C6–C10 in **TS7**. Consequently, attributed to the above two key factors, **TS7** is favored by 3.6 kcal mol^{-1} in free energy than **TS6**, making pathway B unfeasible (the energy surface of pathway B is passed over here as similar to pathway B of the system **III** in Fig. 5, see supporting information for details).

After excluding pathway B, the following D–A reaction of pathway A is also referred to as a great exergonic process, requiring an activation free energy of 25.4 kcal mol^{-1}, relatively higher than that of the model system **I**. The following H-transfer step is shown to be quite different from the model system **I**, in which the ten-membered ring H-transfer assisted by two water molecules is kinetically and thermodynamically favored over the eight-membered ring H-transfer, leading to polycyclic aromatics **4** rather than **13**, which is attributed to a lack of great π conjugation in **TS10** (H-transfer assisted by a water molecule is still disfavored. See supporting information for details). The result is qualitatively consistent with the experimental observation.[5]

For the model system **III**, a sulfur analog of the model system **II**, **5** has two reactive conformers **5-c** and **5-s** as well (Fig. 6). For **5-c**, the geometrically close diyne is very similar to that of **3-c**, while for **5-s**, it is tethered with a smaller angle C7–S8–C9 (101.3°) and longer bonds C7–S8 and S8–C9 (1.85 Å). The conformer **5-s**, served as the more reactive conformer, and is 1.5 kcal mol^{-1} more stable than **5-c**. The change of the angle C2–C3–C4 from 115.6° (**5-c**) to 107.8° (**TS12**) is almost equal to that of C7–S8–C9 from 101.3° (**5-s**) to 93.8° (**TS13**), implying that the two TSs bear similar ring strain. On the other hand, the C1–C5 bond in **TS12** is 2.15 Å, the same as C6–C10 in **TS13**. Accordingly, the activation free energies of ene reactions on both pathways A and B are close (34.1 *versus* 34.5 kcal mol^{-1}, Fig. 5), making them feasible on both sides. Sequentially, pathway A is similar to the model system **II**, leading to the sulfur analog of polycyclic aromatic **6**, while pathway B results in the formation of **6** and thiophene derivative **7**, similar to **2**, once again in complete accord with the experimental result.[5]

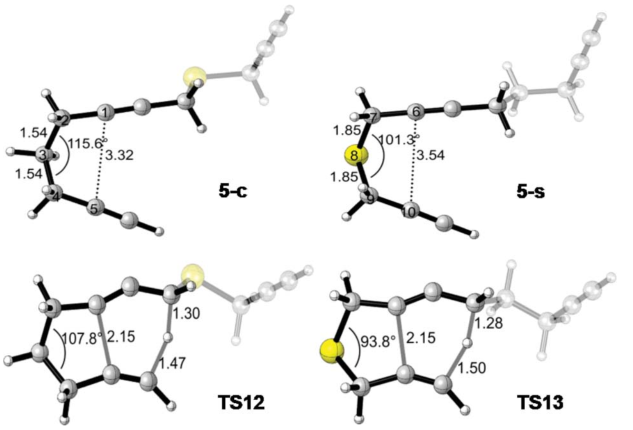

Fig. 6 Transition state structures in model system **III**. Selected distances shown in Å.

The reactions discussed above have illustrated three types of metal-free [2 + 2 + 2] cycloadditions, of which the ene reactions determine the whole reaction rate, and also affect the regioselectivity, while the type of the final product depends on H-transfer during isomerisation. Actually, Roglans' amine-containing macrocyclic triyne system belongs to the model system **I**. For Danheiser's experimental model,[7] the computed energy surface shown in Fig. S2 resembles that in the model system **II**. Although one alkyne is displaced with nitrile as an unactivated functional group in the ene and D–A cycloadditions, the cascade process is still feasible kinetically.

2. Comparison of metal-catalyzed and metal-free reactions

After solving the above-mentioned questions a–d, we focus on why the metal-free cycloaddition can occur through a purely

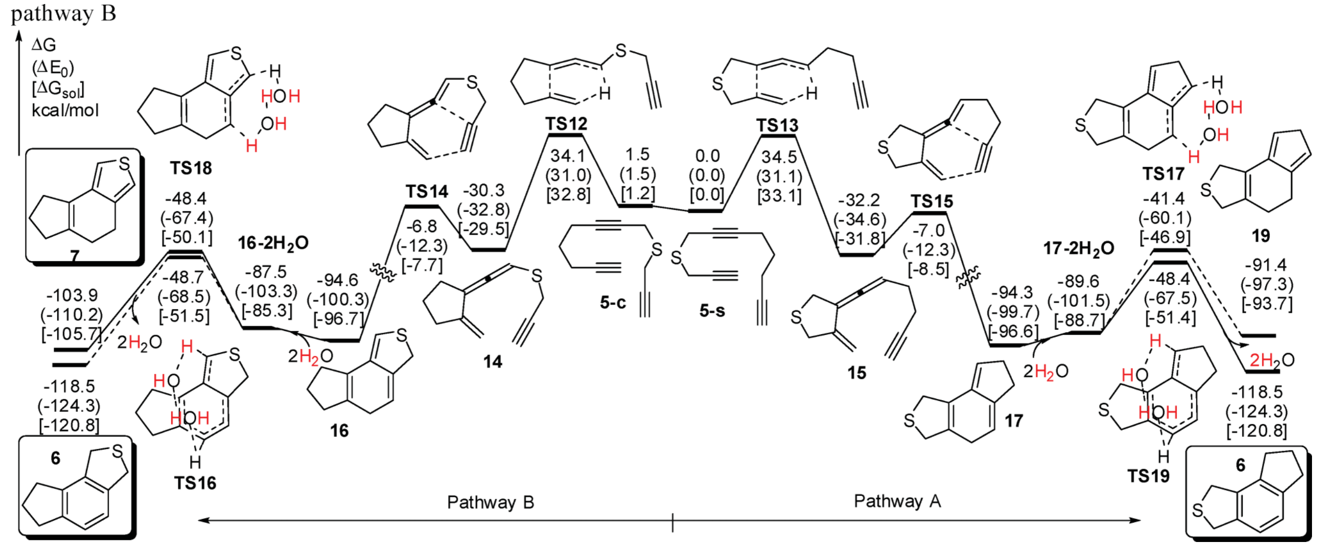

Fig. 5 DFT computed energy surface for the metal-free [2 + 2 + 2] cycloaddition of model system **III**.

thermal process under mild conditions. The distortion/interaction analysis,[14] which is a powerful tool to understand the factors that stabilize the transition states, was employed to allow for deep understanding of the main reasons that allow an increase of the rate of [2 + 2 + 2] cycloaddition without catalysis by transition metals. The activation energy ($\Delta E^{\neq}$) can be mainly separated into the distortion energy of alkynes ($\Delta E^{\neq}_{\text{dist-ynes}}$) and the interaction energy between these distorted reactants ($\Delta E^{\neq}_{\text{int}}$). The transition-metal-catalyzed and metal-free strategies were compared by the distortion/interaction analysis. For the ene reaction of acetylene catalyzed by $CpCoL_2$,[15] there is great acetylene distortion ($\Delta E^{\neq}_{\text{dist-ynes}}$ = 47.0 kcal mol^{-1}) with two acetylenic bonds at the distance of 1.27 Å and a large interaction energy of the two molecules of acetylene ($\Delta E^{\neq}_{\text{int(ynes)}}$ = 26.8 kcal mol^{-1}) with the strong charge repulsion (–0.234 to –0.234, –0.204 to –0.204) observed in the transition state (eqn (1), Fig. 7). Thus, the transition-metal is indeed needed to stabilize the transition state with a significantly low interaction energy between the Co atom and acetylene ($\Delta E^{\neq}_{\text{int(Co-ynes)}}$ = −140.9 kcal mol^{-1}). While for the ene reaction in the metal-free strategy, alkynes incur a minor distortion penalty, resulting from the six-membered ring transition state, and low interaction energy between alkynes ($\Delta E^{\neq}_{\text{int}}$ = –6.3 kcal mol^{-1}) due to weak charge repulsion on C/C (–0.166 to –0.105) and strong charge attraction on C/H/C (–0.872, 0.175 and –0.304), together leading to the metal-free strategy feasible (eqn (3), Fig. 7). In addition, the distortion and interaction energies of monoynes are summed to give the distortion energy in diyne (eqn (2) and (4), Fig. 7). Thus, hepta-1,6-diyne catalyzed by $CpCoL_2$ has a high distortion energy ($\Delta E^{\neq}_{\text{dist(yne)}}$ = 75.5 kcal mol^{-1}), while octa-1,6-diyne undergoes the ene reaction without metal-catalyst with a low distortion energy ($\Delta E^{\neq}_{\text{dist(yne)}}$ = 33.6 kcal mol^{-1}). Consequently, the energy barriers are downhill significantly with metal-catalyst in previous cases, otherwise the reactions cannot work; while the energy barriers in this metal-free strategy are not so high, dominantly attributed to low distortion in the transition state of the ene reaction. The M06-2X method, proved to perform better than B3LYP in calculating the energy barriers of several model catalytic reactions,[16] was also implemented at the same basis set. The results in parentheses indicate that the M06-2X method gives close energies and charges in TS to those obtained from the B3LYP, implying that the B3LYP method can give the correct conclusion.

3. The ene reaction and the cycloaddition involving cyclic ynes

Given its importance, the ene reaction was further investigated (Table 1). Calculations on the size of ring precursors show that the energy level increases as the size gets smaller or bigger even to bimolecular usually catalyzed by metals, which is properly proven in five and six-membered rings (**20–24**).[17] When methylene is replaced by CMe_2[18] or NMe, the energy level decreases slightly (**25**, **27**); when replaced by O (**28**), the energy level is at its lowest point, because the bond length is in the following order: O–C > N–C > C–C and the C–C–C angle is similar to those of C–N–C and C–O–C, making the two alkynes rather close to each other. We also consider the substituent effect on the propargylic and acetylenic positions (Table 1, **30–35** and **36–38**), the energy level slightly reduces in most cases. Though the reaction pathway can be altered by minor differences in energy level, all of which can not be conducted under more mild conditions. After extensive study, to our surprise, diynes involving benzyne (**39** and **40**) can occur through an ene reaction feasibly with a dramatic low activation free energy, which is enlightened by Cheng *et al.*[10c] However, the generated phenylallene appears to be inactive in the subsequent D–A reaction, the activation free energy of which, actually, is not expected to be high (22.3 kcal mol^{-1}, Fig. 8). For further optimizing the model against the above demerit, substrates containing aliphatic cyclic ynes (**41** and **42**) are illuminated by a brilliant idea to aim to decrease the energy barrier of the D–A reaction, which acts as the altered rate-determining step. Indeed, the final designed model system **46** proceeds through the cascade reaction with an overall activation free energy of 19.7 kcal mol^{-1} (Fig. 8), which shows potential to react under very mild conditions; well-rationized cycloalkynes not only activate the π bond of alkynes, but also decrease the distance between the two alkyne moieties in the reacting conformation. Actually, the origin of the feasibility can be also explained by the distortion/interaction model, as the strained cycloalkynes are predicted to be significantly reactive.[19] Thus, the whole reaction system is beneficial to the process with regards to activation.

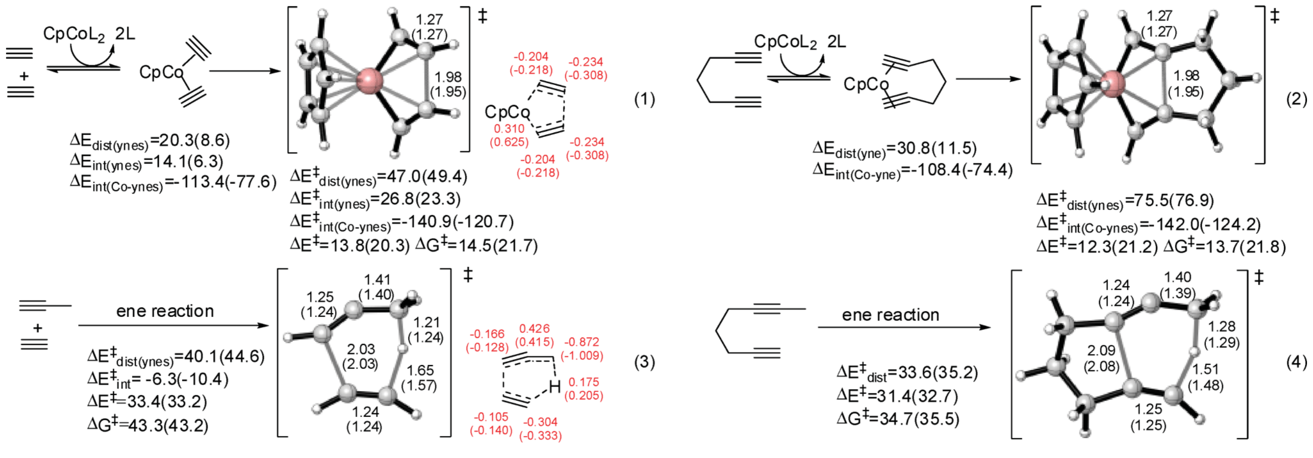

Fig. 7 The distortion/interaction and charge analysis for the transition-metal-catalyzed and metal-free strategies at B3LYP level. Values in parentheses are computed with M06-2X/6-311+(d,p).

Table 1 Energy barriers of intramolecular propargylic ene reactions with different representative diynes

Structure		$\Delta G^{\ddagger}$(TS)/ kcal mol^{-1}	$\Delta H^{\ddagger}$(TS)/ kcal mol^{-1}	$\Delta E^{\ddagger}$(TS)/ kcal mol^{-1}
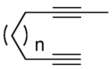	**20** $n = 0$	49.91	46.14	47.30
	21 $n = 1$	34.74	29.97	31.41
	22 $n = 2$	38.48	33.94	35.36
	23 $n = 3$	44.72	40.13	41.53
	24 $n = \infty^{a}$	43.31	32.04	33.35
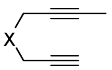	**25** X = CMe_2	32.80	28.66	30.01
	26 X = CO	34.47	30.32	31.59
	27 X = NMe	32.95	28.55	29.92
	28 X = O	31.91	27.16	28.58
	29 X = S	35.52	30.75	32.22
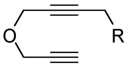	**30** R = Pr	29.37	26.92	27.50
	31 R = Ac	28.79	23.92	25.02
	32 R = Ph	28.44	24.07	25.15
	33 R = acetylenyl	28.34	24.01	25.12
	34 R = F	31.08	26.63	27.84
	35 R = NO_2	29.97	25.39	26.48
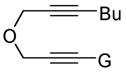	**33** G = CO_2Me	28.74	25.22	26.13
	37 G = Ph	32.84	28.85	29.77
	38 G = C = $CSiMe_3$	29.83	26.43	27.27
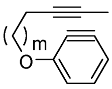	**39** $m = 0$	10.79	7.63	8.45
	40 $m = 1$	11.18	6.75	7.93
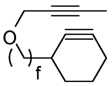	**41** $f = 0$	12.55	8.78	9.83
	42 $f = 1$	16.86	12.34	13.59

[a] Calculated with acetylene and propyne.

Conclusion

In summary, the metal-free and formal [2 + 2 + 2] cycloaddition strategy as a potential methodology for the construction of fused polycyclic compounds has been investigated theoretically in depth with DFT calculations. The present computational studies provide comprehensive understanding on the mechanisms and suggest: a) The present computational studies exclude the diradical mechanism because of high energetic barriers, and support the intramolecular cascade mechanism involving a propargylic ene, Diels–Alder reaction, and water-participated tautomerization. b) The ene reaction acts as the rate-determining step. c) For unsymmetrical triynes or their analogs, the facility of the two yne moieties in participating in the intramolecular propargylic ene reaction is dependent on the tethered atom number (3 > 4 > 5 > 2) and the tethered atom (O > N > C ≈ S). d) Water-assisted H-transfer during tautomerization with favored π conjugation leads to different kinds of products. e) The kinetic feasibility of the metal-free strategy is dominantly attributed to low distortion in the transition state of the ene reaction. f) The different substituents affect the energy barriers slightly. g) Triynes featuring the participation of cyclic ynes were designed and predicted to react under milder conditions with a low energy barrier.

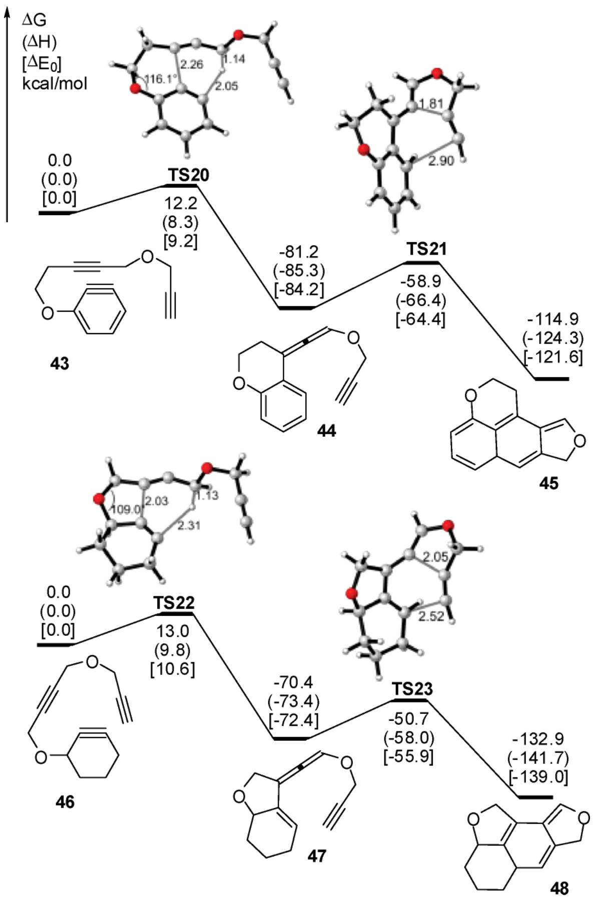

Fig. 8 DFT computed energy surfaces for the metal-free [2 + 2 + 2] cycloaddition of our designed model systems.

Experimental

General method

The optimized geometries and analytical frequencies were calculated at the DFT B3LYP level[20] with 6-311+G(d,p) for all the atoms except the Co atom and LANL2DZ for Co with the Gaussian 03.[21] The transition states were confirmed by the vibrational analysis and characterized by only one imaginary vibrational mode. Intrinsic reaction coordinate (IRC) calculations for the transition state models were performed in order to further obtain the reaction pathways.[22] To explore the impact of the solvent effect on the reaction, the conductor-like polarizable continuum model (CPCM)[23] in toluene was employed. Single-point solvent energy calculations were carried out at the B3LYP/CPCM/6-311+G(d,p) level based on the gas-phase optimized structures. The discussed energies are thermal corrected Gibbs free energies in the gas phase (ΔG) and in solution (ΔG_{sol}). The relative enthalpies (ΔH) and relative energies (ΔE_0) in gas phase are also given. Recently the popular M06-2X[24] hybrid density functional was proved to perform better than B3LYP in calculating the energy barriers of several reactions, the computations were compared with these methods implemented in Gaussian 09.[25] Fig. 2, 4, and 6–8 were prepared using CYLView.[26]

Acknowledgements

The project was supported by National Natural Science Foundation of China (Nos. 20972013 and 20772005), Beijing Natural Science Foundation (No. 2092022), and the Fundamental Research Funds for the Central Universities (Program No. ZZ1020).

Notes and references

1 (*a*) K. P. C. Vollhardt, *Angew. Chem., Int. Ed. Engl.*, 1984, **23**, 539–556; (*b*) N. E. Schore, *Chem. Rev.*, 1988, **88**, 1081–1119; (*c*) N. E. Schore, in *Comprehensive Organic Synthesis*, B. M. Trost, I. Fleming, L. A. Paquette, ed., Pergamon, Oxford, 1991; vol. 5, pp. 1129–1162; (*d*) D. B. Grotjahn, In *Comprehensive Organometallic Chemistry II*, E. W. Abel, F. G. A. Stone, G. Wilkinson, L. S. Hegedus, ed., Pergamon, Oxford, 1995, vol. 12, pp. 741–784; (*e*) M. Lautens, W. Klute and W. Tam, *Chem. Rev.*, 1996, **96**, 49–92; (*f*) I. Ojima, M. Tzamarioudaki, Z. Li and R. J. Donovan, *Chem. Rev.*, 1996, **96**, 635–662; (*g*) H.-W. Frühauf, *Chem. Rev.*, 1997, **97**, 523–596; (*h*) S. Saito and Y. Yamamoto, *Chem. Rev.*, 2000, **100**, 2901–2915; (*i*) M. E. Welker, *Curr. Org. Chem.*, 2001, **5**, 785–807.

2 For recent reviews, see: (*a*) J. A. Varela and C. Saá, *Chem. Rev.*, 2003, **103**, 3787–3801; (*b*) B. Heller and M. Hapke, *Chem. Soc. Rev.*, 2007, **36**, 1085–1094; (*c*) J. A. Varela and C. Saá, *Synlett*, 2008, 2571–2578; (*d*) N. Agenet, O. Buisine, F. Slowinski, V. Gandon, C. Aubert and M. Malacria, *Org. React.*, 2007, **68**, 1–302; (*e*) S. Kotha, E. Brahmachary and K. Lahiri, *Eur. J. Org. Chem.*, 2005, 4741–4767; (*f*) P. R. Chopade and J. Louie,, *Adv. Synth. Catal.*, 2006, **348**, 2307; (*g*) B. R. Galan and T. Rovis, *Angew. Chem., Int. Ed.*, 2009, **48**, 2830–2834; (*h*) K. Tanaka, *Synlett*, 2007, 1977–1993.

3 W. Reppe, O. Schichting, K. Klager and T. Toepel, *Justus Liebigs Ann. Chem.*, 1948, **560**, 1–92.

4 (*a*) V. Breitkopf, H. Hopf, F.-G. Klärner, B. Witulski and B. Zimny, *Liebigs Ann.*, 1995, **100**, 613–617; (*b*) M. G. Kociolek and R. P. Johnson, *Tetrahedron Lett.*, 1999, **40**, 4141–4144; (*c*) D. Rodríguez, L. Castedo, D. Domínguez and C. Saá, *Tetrahedron Lett.*, 1999, **40**, 7701–7704; (*d*) S. Taniguchi, T. Yokoi, A. Izuoka, M. M. Matsushita and T. Sugawara, *Tetrahedron Lett.*, 2004, **45**, 2671–2675.

5 S. Saaby, I. R. Baxendale and S. V. Ley, *Org. Biomol. Chem.*, 2005, **3**, 3365–3368.

6 I. González, A. Pla-Quintana, A. Roglans, A. Dachs, M. Solà, T. Parella, J. Farjas, P. Roura, V. Lloveras and J. Vidal-Gancedo, *Chem. Commun.*, 2010, **46**, 2944–2946.

7 (*a*) J. M. Robinson, T. Sakai, K. Okano, T. Kitawaki and R. L. Danheiser, *J. Am. Chem. Soc.*, 2010, **132**, 11039–11041; (*b*) T. Sakai and R. L. Danheiser, *J. Am. Chem. Soc.*, 2010, **132**, 13203–13205 and references cited therein.

8 P. J. Parsons, A. J. Waters, D. S. Walter and J. Board, *J. Org. Chem.*, 2007, **72**, 1395–1398.

9 For reviews on intramolecular ene reactions, see: (*a*) W. Oppolzer and V. Snieckus, *Angew. Chem., Int. Ed. Engl.*, 1978, **17**, 476–486; (*b*) B. B. Snider, Ene Reactions with Alkenes as Enophiles, in *Comprehensive Organic Synthesis*, L. A. Paquette, Ed., Pergamon Press, Oxford, 1991, Vol. 5, pp 1–28.

10 For ene reactions involving propargylic rather than allylic hydrogen, see: (*a*) W. Oppolzer, E. Pfenninger and J. Keller, *Helv. Chim. Acta*, 1973, **56**, 1807–1812; (*b*) K. J. Shea, L. D. Burke and W. P. England, *Tetrahedron Lett.*, 1988, **29**, 407–410; (*c*) T. T. Jayanth, M. Jeganmohan, M.-J. Cheng, S.-Y. Chu and C.-H. Cheng, *J. Am. Chem. Soc.*, 2006, **128**, 2232–2233; (*d*) M. Altable, S. Filippone, A. Martín-Domenech, M. Güell, M. Solà and N. Martín, *Org. Lett.*, 2006, **8**, 5959–5962; (*e*) D. Peña, D. Pérez, E. Guitián and L. Castedo, *Eur. J. Org. Chem.*, 2003, 1238–1243.

11 For a review on Diels–Alder reactions of vinylallenes, see: M. Murakami, T. Matsuda, Cycloadditions of Allenes, in *Modern Allene Chemistry*, N. Krause, A. S. K. Hashmi, ed., Wiley-VCH, Weinheim, 2004, Vol. 2, pp 727–815.

12 Spin contamination is well known for the calculations of singlet diradical species. The computed energies without or with Yamaguchi–Houk correction for singlet diradical stationary points are all higher than the activation free energies of the corresponding ene reactions (see Supporting Information for details).

13 For theoretical studies on stepwise Diels–Alder reactions, see: (*a*) L. R. Domingo, M. Oliva and J. Andrés, *J. Org. Chem.*, 2001, **66**, 6151–6157; (*b*) H. Wakayama and S. Sakai, *J. Phys. Chem. A*, 2007, **111**, 13575–13582.

14 For recent examples of distortion/interaction analysis in bimolecular reactions: (*a*) D. H. Ess and K. N. Houk, *J. Am. Chem. Soc.*, 2007, **129**, 10646–10647; (*b*) D. H. Ess and K. N. Houk, *J. Am. Chem. Soc.*, 2008, **130**, 10187–10198; (*c*) P. H.-Y. Cheong, R. S. Paton, S. M. Bronner, G.-Y. Im, N. K. Garg and K. N. Houk, *J. Am. Chem. Soc.*, 2010, **132**, 1267–1269; (*d*) P. Liu, P. McCarren, P. H. Cheong, T. F. Jamison and K. N. Houk, *J. Am. Chem. Soc.*, 2010, **132**, 2050–2057; (*e*) Y. Lan and K. N. Houk, *J. Am. Chem. Soc.*, 2010, **132**, 17921–17927 and references cited therein.

15 V. Gandon, N. Agenet, K. P. C. Vollhardt, M. Malacria and C. Aubert, *J. Am. Chem. Soc.*, 2006, **128**, 8509–8520 and references cited therein.

16 K. Yang, J. Zheng, Y. Zhao and D. G. Truhlar, *J. Chem. Phys.*, 2010, **132**, 164117.

17 For the unsymmetrical triynes with five and six-member ring precursors, see Fig. S3 in the Supporting Information.

18 For *gem*-dimethyl effect, see: M. E. Jung and G. Piizi, *Chem. Rev.*, 2005, **105**, 1735–1766.

19 For the recent calculations on cycloalkynes with distortion/interaction analysis, see: F. Schoenebeck, D. H. Ess, G. O. Jones and K. N. Houk, *J. Am. Chem. Soc.*, 2009, **131**, 8121–8133 and references cited therein.

20 (*a*) A. D. Becke, *J. Chem. Phys.*, 1993, **98**, 5648–5652; (*b*) C. Lee, W. Yang and R. G. Parr, *Phys. Rev. B*, 1988, **37**, 785–789.

21 M. J. Frisch, G. W. Trucks, H. B. Schlegel, G. E. Scuseria, M. A. Robb, J. R. Cheeseman, J. A. Montgomery Jr., T. Vreven, K. N. Kudin, J. C. Burant, J. M. Millam, S. S. Iyengar, J. Tomasi, V. Barone, B. Mennucci, M. Cossi, G. Scalmani, N. Rega, G. A. Petersson, H. Nakatsuji, M. Hada, M. Ehara, K. Toyota, R. Fukuda, J. Hasegawa, M. Ishida, T. Nakajima, Y. Honda, O. Kitao, H. Nakai, M. Klene, X. Li, J. E. Knox, H. P. Hratchian, J. B. Cross, C. Adamo, J. Jaramillo, R. Gomperts, R. E. Stratmann, O. Yazyev, A. J. Austin, R. Cammi, C. Pomelli, J. W. Ochterski, P. Y. Ayala, K. Morokuma, G. A. Voth, P. Salvador, J. J. Dannenberg, V. G. Zakrzewski, S. Dapprich, A. D. Daniels, M. C. Strain, O. Farkas, D. K. Malick, A. D. Rabuck, K. Raghavachari, J. B. Foresman, J. V. Ortiz, Q. Cui, A. G. Baboul, S. Clifford, J. Cioslowski, B. B. Stefanov, G. Liu, A. Liashenko, P. Piskorz, I. Komaromi, R. L. Martin, D. J. Fox, T. Keith, M. A. Al-Laham, C. Y. Peng, A. Nanayakkara, M. Challacombe, P. M. W. Gill, B. Johnson, W. Chen, M. W. Wong, C. Gonzalez and J. A. Pople, *Gaussian 03*, Revision C.02; Gaussian, Inc., Wallingford, CT, 2004.

22 (*a*) K. Fukui, *J. Phys. Chem.*, 1970, **74**, 4161–4163; (*b*) K. Ishida, K. Morokuma and A. Komornicki, *J. Chem. Phys.*, 1977, **66**, 2153–2156; (*c*) C. González and H. B. Schlegel, *J. Phys. Chem.*, 1990, **94**, 5523–5527.

23 (*a*) V. Barone and M. Cossi, *J. Phys. Chem. A*, 1998, **102**, 1995–2001; (*b*) M. Cossi, N. Rega, G. Scalmani and V. Barone, *J. Comput. Chem.*, 2003, **24**, 669–681; (*c*) Y. Takano and K. N. Houk, *J. Chem. Theory Comput.*, 2005, **1**, 70–77.

24 Y. Zhao and D. G. Truhlar, *Theor. Chem. Acc.*, 2008, **120**, 215–241.

25 M. J. Frisch, G. W. Trucks, H. B. Schlegel, G. E. Scuseria, M. A. Robb, J. R. Cheeseman, G. Scalmani, V. Barone, B. Mennucci, G. A. Petersson, H. Nakatsuji, M. Caricato, X. Li, H. P. Hratchian, A. F. Izmaylov, J. Bloino, G. Zheng, J. L. Sonnenberg, M. Hada, M. Ehara, K. Toyota, R. Fukuda, J. Hasegawa, M. Ishida, T. Nakajima, Y. Honda, O. Kitao, H. Nakai, T. Vreven, J. A. Montgomery Jr., J. E. Peralta, F. Ogliaro, M. Bearpark, J. J. Heyd, E. Brothers, K. N. Kudin, V. N. Staroverov, R. Kobayashi, J. Normand, K. Raghavachari, A. Rendell, J. C. Burant, S. S. Iyengar, J. Tomasi, M. Cossi, N. Rega, J. M. Millam, M. Klene, J. E. Knox, J. B. Cross, V. Bakken, C. Adamo, J. Jaramillo, R. Gomperts, R. E. Stratmann, O. Yazyev, A. J. Austin, R. Cammi, C. Pomelli, J. W. Ochterski, R. L. Martin, K. Morokuma, V. G. Zakrzewski, G. A. Voth, P. Salvador, J. J. Dannenberg, S. Dapprich, A. D. Daniels, Ö. Farkas, J. B. Foresman, J. V. Ortiz, J. Cioslowski and D. J. Fox, *Gaussian 09*, Revision A.01, Gaussian, Inc., Wallingford CT, 2009.

26 C. Y. Legault, *CYLView, 1.0b*, Université de Sherbrooke, Québec, Montreal, Canada, 2009, http://www.cylview.org.